

---

# STRUCTURE-PRESERVING REDUCED-ORDER MODELLING OF KORTEWEG-DE VRIES EQUATION

---

A PREPRINT

**Murat Uzunca**

Department of Mathematics, Sinop University  
Sinop-Turkey  
muzunca@sinop.edu.tr

**Süleyman Yıldız**

Institute of Applied Mathematics  
Middle East Technical University, Ankara-Turkey  
yildiz.suleyman@metu.edu.tr

**Bülent Karasözen**

Institute of Applied Mathematics & Department of Mathematics, Middle East Technical University  
Ankara-Turkey  
bulent@metu.edu.tr

February 9, 2021

## ABSTRACT

Computationally efficient, structure-preserving reduced-order methods are developed for the Korteweg-de Vries (KdV) equations in Hamiltonian form. The semi-discretization in space by finite differences is based on the Hamiltonian structure. The resulting skew-gradient system of ordinary differential equations (ODEs) is integrated with the linearly implicit Kahan's method, which preserves the Hamiltonian approximately. We have shown, using proper orthogonal decomposition (POD), the Hamiltonian structure of the full-order model (FOM) is preserved by the reduced-order model (ROM). The reduced model has the same linear-quadratic structure as the FOM. The quadratic nonlinear terms of the KdV equations are evaluated efficiently by the use of tensorial framework, clearly separating the offline-online cost of the FOMs and ROMs. The accuracy of the reduced solutions, preservation of the conserved quantities, and computational speed-up gained by ROMs are demonstrated for the one-dimensional single and coupled KdV equations, and two-dimensional Zakharov-Kuznetsov equation with soliton solutions.

**Keywords** Hamiltonian systems, solitary waves, Kahan's method, energy preservation, model order reduction, tensor algebra

Mathematics Subject Classification 2010: 65P10, 65L05, 34C20, 15A69

## 1 Introduction

Numerical integration of large scale dynamical systems is computationally costly and requires a large amount of computer memory for applications in real-time and many query solutions. The reduced-order methods (ROMs) have emerged as a powerful approach to reduce the computational effort by constructing a low-dimensional linear subspace, that approximately represents the solution to the high-dimensional system [Benner et al.(2017)Benner, Cohen, Ohlberger, and Willcox, Quarteroni and Rozza(2014), Hesthaven et al.(2016)Hesthaven, Rozza, and Stamm]. Projection-based model reduction is one of the well-known and widely used ROM techniques, generally implemented using offline-online decomposition. Proper orthogonal decomposition (POD) with Galerkin projection is one of the most standard methods to construct a reduced basis [Berkooz et al.(1993)Berkooz, Holmes, and Lumley, Sirovich(1987)]. During the offline stage, a set of reduced basis is extracted from a collection of high-fidelity solutions. In the online stage, the reduced solutions are computed in the reduced space, spanned by a set of basis functions that represents the main dynamics of the full-order model (FOM).

Many dynamical systems have some mathematical structures, such as symmetry, symplecticity, and energy preservation. Numerical integrators that inherit such properties are referred to as geometric numerical integrators or structure-preserving integrators [Hairer et al.(2016)Hairer, Lubich, and Wanner]. They produce stable and qualitatively better numerical solutions than standard general-purpose integrators. Various symplectic and multisymplectic algorithms have been extended to Hamiltonian partial differential equations (PDEs) to preserve conservation laws. When a Hamiltonian PDE is considered, the Galerkin projection-based POD-ROM is not able to preserve the desired physical quantities of the original system because the Hamiltonian structure of the original system may not be retained in the reduced dynamical system. The reduced-order solutions may exhibit spurious and unphysical artifacts, leading to instabilities and qualitatively wrong solution behavior. Therefore, ROMs are preferred, that preserve the geometric structure and conserved quantities of FOMs. In the recent years, several structure-preserving reduced-order methods have been developed for Lagrangian systems [Carlberg et al.(2013)Carlberg, Farhat, Cortial, and Amsallem], for port-Hamiltonian systems [Chaturantabut et al.(2016)Chaturantabut, Beattie, and Gugercin], for dissipative Hamiltonian systems [Afkham and Hesthaven(2019)], for canonical [Afkham and Hesthaven(2017), Buchfink et al.(2019)Buchfink, Bhatt, and Haasdonk, Hesthaven and Pagliantini(2020), Peng and Mohseni(2016), Karasözen and Uzunca(2018)], and for non-canonical Hamiltonian PDEs [Gong et al.(2017)Gong, Wang, and Wang, Miyatake(2019), Hesthaven and Pagliantini(2018)].

In this paper, we develop an efficient structure-preserving ROMs for the Korteweg-de Vries (KdV) equation. The KdV equation is an integrable Hamiltonian PDE with a constant Poisson structure. The conserved quantities of the KdV equation are the cubic Hamiltonian (energy), quadratic momentum and linear mass. The KdV equation is a nonlinear dispersive equation with smooth solutions. There are relatively few papers concerning reduced-order modeling of the KdV equation. In [Gerbeau and Lombardi(2014)] ROMs are constructed based on Lax-pairs, and in [Hesthaven and Pagliantini(2018)] a greedy POD algorithm is developed with discrete empirical interpolation method (DEIM) based on the Poisson structure. In [Miyatake(2019)] structure-preserving POD and DEIM are constructed preserving first integrals of the KdV equation, and in [Ehrlacher et al.(2020)Ehrlacher, Lombardi, Mula, and Vialárd] for one-dimensional conservative PDEs in Wasserstein space, ROMs are constructed including the KdV equation. For nonlinear PDEs without polynomial structure, using hyper-reduction methods like the empirical interpolation (EIM) [Barrault et al.(2004)Barrault, Maday, Nguyen, and Patera] and DEIM [Chaturantabut and Sorensen(2010)], the computational efficiency is discovered in solving the reduced system, i.e., in the online stage. When nonlinear PDEs like the KdV equation have polynomial structure, projecting the FOM onto the reduced space yields low-dimensional matrix operators that preserve the polynomial structure of the FOMs. Using the offline-online decomposition, computationally efficient ROMs can be constructed.

The KdV equation is discretized in space using various methods; finite difference, finite-volume, finite-element, spectral elements. Finite-volume and finite-element methods are suited for complex geometries, while spectral methods have higher order accuracy, but lead to dense matrices for two-dimensional problems. Here, we consider only one-dimensional and rectangular two-dimensional domains in space. In this paper, we discretize the KdV equation in space by finite differences while preserving the skew-symmetry of the Poisson structure. The resulting skew-gradient system of ordinary differential equations (ODEs) preserves the energy, momentum, and mass at the discrete level. The resulting semi-discrete system is a linear-quadratic ODE system. Most of the energy-preserving methods proposed so far are fully implicit methods, like the average vector field (AVF) method [Celledoni et al.(2012)Celledoni, Grimm, McLachlan, McLaren, O’Neale, Owren, and Quispel], where a system of nonlinear equations has to be solved at each time step by iterative methods like Newton’s method or fixed-point iteration. The computational cost of the iterative solvers increases with the number of iterations and system size. The AVF method also requires the use of hyper-reduction techniques such as the DEIM to reduce the computational cost of the nonlinear terms in the ROMs [Karasözen and Uzunca(2018)]. For time discretization, we use as an alternative to AVF, the second-order linearly implicit Kahan’s method [Kahan and Li(1997), Celledoni et al.(2013)Celledoni, McLachlan, Owren, and Quispel] which is designed for ODEs with quadratic polynomial terms, obtained by semi-discretization of the KdV equation in space by finite differences. In contrast to the fully implicit energy preserving schemes such as the average vector field (AVF) method and the mid-point method, Kahan’s method requires only one step Newton iteration at each time step for linear-quadratic systems such as the semi-discrete KdV equation [Celledoni et al.(2013)Celledoni, McLachlan, Owren, and Quispel]. Kahan’s method preserves the cubic integrals such as the Hamiltonians at the discrete-time level [Celledoni et al.(2015)Celledoni, McLachlan, McLaren, Owren, and Quispel]. Applying POD in the tensorial framework (TPOD) [Benner et al.(2018)Benner, Goyal, and Gugercin, Benner and Breiten(2015), Kramer and Willcox(2019)] by exploiting matricizations of tensors, the TPOD-ROM for the KdV equation with quadratic nonlinearity recovers an efficient offline-online decomposition. The offline computation is accelerated by the use of tensor techniques like matricizations of tensors [Benner and Breiten(2015), Benner et al.(2018)Benner, Goyal, and Gugercin, Benner and Goyal(2021), Kramer and Willcox(2019)]. Here we make use of the sparse matrix technique MULTIPROD [Leva(2008)] to further speed up the tensor calculations in

the offline stage. We show the computational efficiency of the TPOD for three different KdV equations with soliton solutions; the one-dimensional single and coupled KdV equations, and the Zakharov-Kuznetsov equation which is a two-dimensional KdV equation.

The paper organized as follows. In Section 2 we introduce the FOM for three types of the KdV equations. In Section 3 the structure-preserving ROMs with POD and TPOD are developed. We present in Section 4 numerical experiments demonstrating the preservation of the invariants accurately by ROMs with a low computational cost. The paper ends with concluding remarks in Section 5. Through the paper, variables are denoted by plain letters, vectors are denoted by bold letters, and matrices and tensors are denoted by capital letters.

## 2 Full-order model

KdV equation is a dispersive, nonlinear hyperbolic equation with smooth solutions. It describes the propagation of long, one-dimensional waves, including shallow-water waves, long internal waves in the ocean, ion-acoustic waves in a plasma, acoustic waves on a crystal lattice, and more. Dispersion and non-linearity can interact to produce permanent and localized waveforms. The KdV equation is a Hamiltonian PDE with a constant Poisson structure. It possesses bi-Hamiltonian structure [Nutku and Oğuz(1990), Karasözen and Şimşek(2013)], i.e., there exists an infinite number of invariants and therefore it is completely integrable. It was solved using various geometric integrators; symplectic and multisymplectic methods [Ascher and McLachlan(2005), Chen et al.(2011)Chen, Song, and Zhu, Bridges and Reich(2001)], energy preserving integrators [Karasözen and Şimşek(2013), Eidnes and Li(2020), Karasözen and Şimşek(2012)]. In this section, we construct FOMs by discretizing the one-dimensional single and coupled KdV equations, and the two-dimensional KdV equation, i.e., Zakharov-Kuznetsov equation, in space and time.

### 2.1 Single KdV equation

The one-dimensional KdV equation is given as

$$\partial_t u = -\alpha u \partial_x u - \mu \partial_{xxx} u, \quad (1)$$

in a space-time domain  $[a, b] \times [0, T]$  ( $a < b$ ,  $T > 0$ ), with an initial condition and the periodic boundary condition

$$u(x, 0) = u^0(x), \quad u(a, t) = u(b, t),$$

with the real parameters  $\alpha$  and  $\mu$ . The KdV equation (1) can be written as a Hamiltonian PDE of the following form

$$\partial_t u = \mathcal{S} \frac{\delta \mathcal{H}}{\delta u},$$

where  $\delta$  and  $\partial$  denote the variational derivative and partial derivative, respectively. The constant skew-adjoint operator (Poisson tensor)  $\mathcal{S}$  and the Hamiltonian functional  $\mathcal{H}$  are given by

$$\mathcal{S} = \partial_x, \quad \mathcal{H}(u) = \int_a^b \left( -\frac{\alpha}{6} u^3 + \frac{\mu}{2} (\partial_x u)^2 \right) dx.$$

The KdV equation (1) is completely integrable, i.e., it has infinitely many invariants. Among them, the momentum  $\mathcal{I}_1 = \int u^2 dx$ , and the mass  $\mathcal{I}_2 = \int u dx$  are the most important ones.

Semi-discrete form of the KdV equation is obtained on the partition of the spatial interval  $[a, b]$  into  $N_x$  uniform elements

$$a = x_1 < x_2 < \dots < x_{N_x} < x_{N_x+1} = b, \quad \Delta x = (b - a)/(N_x).$$

Then we set semi-discrete solution vector as  $\mathbf{u} := \mathbf{u}(t) = (u_1(t), \dots, u_{N_x}(t))^T$ , where  $u_i(t) = u(x_i, t)$ ,  $i = 1, \dots, N_x$ . The discrete Hamiltonian  $H(\mathbf{u})$  is given by

$$H(\mathbf{u}) = \sum_{i=1}^{N_x} \left( -\frac{\alpha}{6} u_i^3 + \frac{\mu}{2} \left( \frac{u_{i+1} - u_i}{\Delta x} \right)^2 \right) \Delta x. \quad (2)$$

Similarly, the discrete momentum and mass are given as

$$I_1(\mathbf{u}) = \sum_{i=1}^{N_x} u_i^2 \Delta x, \quad I_2(\mathbf{u}) = \sum_{i=1}^{N_x} u_i \Delta x.$$

The semi-discretized KdV equation (1) is a Hamiltonian system of ODEs, equivalently a skew-gradient system

$$\mathbf{u}_t = S \nabla H(\mathbf{u}), \quad (3)$$

with the discrete gradient  $\nabla H(\mathbf{u})$  and the constant skew-symmetric matrix  $S$

$$\nabla H(\mathbf{u}) = -\frac{\alpha}{2} \mathbf{u} \odot \mathbf{u} - \mu D_2 \mathbf{u}, \quad S = D_1,$$

where  $\odot$  denotes the element-wise multiplication of vectors. The matrices  $D_1 \in \mathbb{R}^{N_x \times N_x}$  and  $D_2 \in \mathbb{R}^{N_x \times N_x}$  correspond to the centred finite difference discretization of the first and second order derivative operators  $\partial_x$  and  $\partial_{xx}$ , respectively, which are given under periodic boundary conditions by

$$D_1 := \frac{1}{2\Delta x} \begin{pmatrix} 0 & 1 & & -1 \\ -1 & 0 & 1 & \\ & \ddots & \ddots & \ddots \\ & & -1 & 0 & 1 \\ 1 & & & -1 & 0 \end{pmatrix}, \quad D_2 := \frac{1}{\Delta x^2} \begin{pmatrix} -2 & 1 & & & 1 \\ 1 & -2 & 1 & & \\ & \ddots & \ddots & \ddots & \\ & & & 1 & -2 & 1 \\ 1 & & & & 1 & -2 \end{pmatrix}, \quad (4)$$

where  $D_1$  is skew-symmetric as an approximation of the skew-adjoint Poisson tensor  $\mathcal{S}$ . Then, the semi-discretized KdV equation (1) can be written as

$$\mathbf{u}_t = - \underbrace{\mu D_3 \mathbf{u}}_{\text{linear}} - \underbrace{\frac{\alpha}{2} D_1 (\mathbf{u} \odot \mathbf{u})}_{\text{quadratic}}, \quad (5)$$

where the skew-symmetric matrix  $D_3 := D_1 D_2$  approximates the third order derivative  $\partial_{xxx}$ .

For time discretization, we divide the time interval  $[0, T]$  into  $N_t$  uniform elements  $0 = t_0 < t_1 < \dots < t_{N_t} = T$ ,  $\Delta t = T/N_t$ , and we denote by  $\mathbf{u}^k = \mathbf{u}(t_k)$  the full discrete approximation vector at time  $t_k$ ,  $k = 0, \dots, N_t$ . The semi-discrete KdV equation (5) is a linear-quadratic system of ODEs of the following form

$$\mathbf{u}_t = \mathbf{f}(\mathbf{u}) := B_q Q(\mathbf{u}) + B_l \mathbf{u}, \quad (6)$$

with the quadratic vector field  $Q(\mathbf{u}) = (\mathbf{u} \odot \mathbf{u})$  and the skew-symmetric matrices  $B_l = -\mu D_3$  and  $B_q = (-\alpha/2) D_1$ . As the time integrator, we use Kahan's method [Celledoni et al.(2012)Celledoni, Grimm, McLachlan, McLaren, O'Neale, Owren, and Quispel, Kahan and Li(1997)] whose application to the linear-quadratic system (6) yields

$$\frac{\mathbf{u}^{k+1} - \mathbf{u}^k}{\Delta t} = B_q \tilde{Q}(\mathbf{u}^k, \mathbf{u}^{k+1}) + \frac{1}{2} B_l (\mathbf{u}^k + \mathbf{u}^{k+1}),$$

where the symmetric bilinear form  $\tilde{Q}(\cdot, \cdot)$  is obtained by the polarization of the quadratic vector field  $Q(\cdot)$  as follows [Celledoni et al.(2015)Celledoni, McLachlan, McLaren, Owren, and Quispel]

$$\tilde{Q}(\mathbf{u}^k, \mathbf{u}^{k+1}) := \frac{1}{2} (Q(\mathbf{u}^k + \mathbf{u}^{k+1}) - Q(\mathbf{u}^k) - Q(\mathbf{u}^{k+1})).$$

For a large class of Hamiltonian systems, the method has a conserved quantity (related to energy) and an invariant [Kahan and Li(1997), Sanz-Serna(1994)]. Kahan's method is second order, time-reversal, and linearly implicit for ODEs with quadratic vector fields [Celledoni et al.(2013)Celledoni, McLachlan, Owren, and Quispel] like the semi-discrete KdV equation (6), i.e.,  $\mathbf{u}^{k+1}$  can be computed by solving a single linear system of equations

$$\left( I - \frac{\Delta t}{2} \mathbf{f}'(\mathbf{u}^k) \right) \tilde{\mathbf{u}} = \Delta t \mathbf{f}(\mathbf{u}^k), \quad \mathbf{u}^{k+1} = \mathbf{u}^k + \tilde{\mathbf{u}},$$

where  $I$  is the identity matrix and  $\mathbf{f}'$  denotes the Jacobian matrix of  $\mathbf{f}$ .

Kahan's method is the restriction of a Runge-Kutta method to quadratic vector fields [Celledoni et al.(2013)Celledoni, McLachlan, Owren, and Quispel]

$$\frac{\mathbf{u}^{k+1} - \mathbf{u}^k}{\Delta t} = -\frac{1}{2} \mathbf{f}(\mathbf{u}^k) + 2 \mathbf{f} \left( \frac{\mathbf{u}^{k+1} + \mathbf{u}^k}{2} \right) - \frac{1}{2} \mathbf{f}(\mathbf{u}^{k+1}). \quad (7)$$

Kahan's method preserves the Hamiltonian approximately, i.e., it preserves the modified Hamiltonian or the polarized energy

$$\tilde{H}(\mathbf{u}) := H(\mathbf{u}) + \frac{1}{2} \Delta t \nabla H(\mathbf{u})^T \left( I - \frac{1}{2} \Delta t \mathbf{f}'(\mathbf{u}) \right)^{-1} \mathbf{f}(\mathbf{u}),$$

for all cubic Hamiltonian systems with constant Poisson structure such as the KdV equation [Celledoni et al.(2013)Celledoni, McLachlan, Owren, and Quispel].

Kahan's method has not been extensively studied for solving PDEs so far, with the exception [Kahan and Li(1997)], where it is applied for solving the KdV equation. It was shown that Kahan's method exhibits all favorable numerical properties like energy conservation, linear error growth with time. For Hamiltonian PDEs, using multiple points to discretize the variational derivative, linearly implicit energy-preserving schemes are defined [Matsuo and Furihata(2001)]. These methods are generalized for deriving linearly implicit energy-preserving multistep methods for Hamiltonian PDEs with polynomial invariants [Dahlby and Owren(2011)]. A comparison of this approach and Kahan's method applied to PDEs is given in [Eidnes et al.(2019)Eidnes, Li, and Sato]. Recently a two-step generalization of Kahan's method [Eidnes and Li(2020)] is applied to multisymplectic PDEs with cubic invariants. It was shown that discrete approximations to local and global energy conservation laws are preserved for the one-dimensional KdV equation and the two-dimensional Zakharov-Kuznetsov equation.

Other energy preserving integrators like the implicit mid-point rule [Miyatake(2019)] and the AVF method [Hesthaven and Pagliantini(2018)], both are applied to the KdV equation in the context of reduced-order modelling, are fully implicit. The resulting nonlinear algebraic equations have to be solved by iteratively. We remark that implicit mid-point rule preserves only the quadratic Hamiltonians, whereas the AVF method preserves cubic Hamiltonians. For two-dimensional problems, where fully implicit schemes are computationally costly, the linearly implicit methods seem to provide for a competitive method. The full order solutions can be speeded up in the periodic setting using the slit-step fast Fourier transformation (FFT) method which was originally proposed in [Hardin(1973)].

## 2.2 Coupled KdV equation

As the second model, we consider the one-dimensional symmetric coupled KdV-KdV system [Karasözen and Şimşek(2012), Bona et al.(2007)Bona, Dougalis, and Mitsotakis]

$$\begin{aligned}\partial_t u &= \frac{3}{2}u\partial_x u - \frac{1}{2}v\partial_x v - \partial_x v - \frac{1}{6}\partial_{xxx}v, \\ \partial_t v &= -\partial_x u - \frac{1}{2}\partial_x(uv) - \frac{1}{6}\partial_{xxx}u,\end{aligned}\tag{8}$$

which represents approximation to two-dimensional Euler equations for surface water waves propagation along a horizontal channel, where  $u$  is the horizontal velocity and  $v$  is the deviation of the free surface from its rest position  $x$ . The initial and periodic boundary conditions are

$$u_0(x, t) = u^0(x), \quad v_0(x, t) = v^0(x), \quad u(a, t) = u(b, t), \quad v(a, t) = v(b, t).$$

The corresponding Hamiltonian and skew-adjoint Poisson tensor for the KdV-KdV system (8) are given by

$$\mathcal{H}(u, v) = \int_a^b \left( -uv - \frac{1}{4}uv^2 - \frac{1}{4}u^3 - \frac{1}{6}u\partial_{xx}v \right) dx, \quad \mathcal{S} = \begin{pmatrix} \partial_x & 0 \\ 0 & \partial_x \end{pmatrix}.$$

Additional invariants for the coupled KdV-KdV system (8) are the momentum  $\mathcal{I}_1 = \int (u^2 + v^2)dx$ , and the masses  $\mathcal{I}_2 = \int u dx$  and  $\mathcal{I}_3 = \int v dx$ . The discrete Hamiltonian  $H(\mathbf{u}, \mathbf{v})$  is given by

$$H(\mathbf{u}, \mathbf{v}) = \sum_{i=1}^{N_x} \left( -u_i v_i - \frac{1}{4}u_i v_i^2 - \frac{1}{4}u_i^3 - \frac{1}{6}u_i \left( \frac{v_{i+1} - 2v_i + v_{i-1}}{\Delta x^2} \right) \right) \Delta x.\tag{9}$$

The semi-discrete form of the coupled KdV-KdV system (8) can be written as a skew-gradient system with linear and quadratic terms

$$\begin{aligned}\mathbf{u}_t &= - \underbrace{\left( D_1 + \frac{1}{6}D_3 \right)}_{\text{linear}} \mathbf{v} - \underbrace{\frac{3}{4}D_1(\mathbf{u} \odot \mathbf{u}) - \frac{1}{4}D_1(\mathbf{v} \odot \mathbf{v})}_{\text{quadratic}}, \\ \mathbf{v}_t &= - \underbrace{\left( D_1 + \frac{1}{6}D_3 \right)}_{\text{linear}} \mathbf{u} - \underbrace{\frac{1}{2}D_1(\mathbf{u} \odot \mathbf{v})}_{\text{quadratic}}.\end{aligned}\tag{10}$$

## 2.3 Zakharov-Kuznetsov equation

The third model is the two-dimensional (2D) KdV equation known as the Zakharov-Kuznetsov equation [Iwasaki et al.(1990)Iwasaki, Toh, and Kawahara, Nishiyama et al.(2012)Nishiyama, Noi, and Oharu,

Zakharov and Kuznetsov(1974), Xu and Shu(2005)]

$$\partial_t u = -\alpha u \partial_x u - \mu(\partial_{xxx} u - \partial_{xyy} u), \quad (11)$$

in the space-time domain  $([a, b] \times [c, d]) \times [0, T]$  ( $a < b$ ,  $c < d$ ,  $T > 0$ ) with the initial condition and periodic boundary conditions

$$u(x, y, 0) = u^0(x, y), \quad u(a, y, t) = u(b, y, t), \quad u(x, c, t) = u(x, d, t).$$

The skew-adjoint Poisson tensor and Hamiltonian are given as

$$\mathcal{S} = \partial_x, \quad \mathcal{H}(u) = \int_c^d \int_a^b \left( -\frac{\alpha}{6} u^3 + \frac{\mu}{2} ((\partial_x u)^2 + (\partial_y u)^2) \right) dx dy. \quad (12)$$

Additional invariants are the momentum  $I_1 = \iint \frac{1}{2} u^2 dx dy$  and the mass  $I_2 = \iint u dx dy$ . It describes the motion of nonlinear ion-acoustic waves in magnetized plasma.

For space discretization, the spatial domain  $\Omega = [a, b] \times [c, d]$  is divided into  $N_x$  and  $N_y$  elements in  $x$  and  $y$  directions, respectively, to form a rectangular mesh

$$\begin{aligned} a = x_1 < x_2 < \dots < x_{N_x} < x_{N_x+1} = b, & \quad \Delta x = (b - a)/(N_x), \\ c = y_1 < y_2 < \dots < y_{N_y} < y_{N_y+1} = d, & \quad \Delta y = (d - c)/(N_y). \end{aligned}$$

Then, the semi-discrete solution vector is defined as

$$\mathbf{u} := \mathbf{u}(t) = (u_{1,1}(t), \dots, u_{1,N_y}(t), u_{2,1}(t), \dots, u_{N_x,N_y}(t))^T,$$

where  $u_{i,j}(t) = u(x_i, y_j, t)$ ,  $i = 1, \dots, N_x$ ,  $j = 1, \dots, N_y$ . The discrete form of the Hamiltonian in (12) is given by

$$H(\mathbf{u}) = \sum_{i=1}^{N_x} \sum_{j=1}^{N_y} \left( -\frac{1}{6} (u_{i,j})^3 + \frac{\mu}{2} \left( \frac{u_{i+1,j} - u_{i,j}}{\Delta x} \right)^2 + \frac{\mu}{2} \left( \frac{u_{i,j+1} - u_{i,j}}{\Delta y} \right)^2 \right) \Delta x \Delta y. \quad (13)$$

The semi-discrete form of the Zakharov-Kuznetsov equation (11) is a skew-gradient system of the form

$$\begin{aligned} \mathbf{u}_t &= S \nabla H(\mathbf{u}) = D_x \left( -\frac{\alpha}{2} (\mathbf{u} \odot \mathbf{u}) - \mu (D_{xx} + D_{yy}) \mathbf{u} \right) \\ &= \underbrace{-\mu (D_{xxx} + D_{xyy}) \mathbf{u}}_{\text{linear}} - \underbrace{\frac{\alpha}{2} D_x (\mathbf{u} \odot \mathbf{u})}_{\text{quadratic}}, \end{aligned} \quad (14)$$

where we set  $D_{xxx} := D_x D_{xx}$ ,  $D_{xyy} := D_x D_{yy}$ , and the 2D centred finite difference matrices  $D_x, D_{xx}, D_{yy} \in \mathbb{R}^{N_x N_y \times N_x N_y}$  are defined by

$$D_x = D_1 \otimes I_y, \quad D_{xx} = D_2 \otimes I_y, \quad D_{yy} = I_x \otimes D_2,$$

where  $I_x$  and  $I_y$  are  $N_x$  and  $N_y$  dimensional identity matrices, and the matrices  $D_1$  and  $D_2$  are the ones defined in (4), with appropriate dimension.

### 3 Reduced-order model

Semi-discretization of KdV equations in Section 2 leads to the following system of linear-quadratic ODEs

$$\frac{d\mathbf{q}}{dt} = S \nabla_{\mathbf{q}} H(\mathbf{q}) = B_l \mathbf{q} + B_q Q(\mathbf{q}), \quad (15)$$

where  $\mathbf{q} \in \mathbb{R}^N$  is the state vector,  $B_l, B_q \in \mathbb{R}^{N \times N}$  are the linear operators,  $Q(\mathbf{q}) : \mathbb{R}^N \rightarrow \mathbb{R}^N$  is the quadratic operator, and  $N$  is the degree of freedom of the system, where  $N = N_x$  for the single KdV system (5),  $N = 2N_x$  for the coupled KdV system (10), and  $N = N_x \times N_y$  for the Zakharov-Kuznetsov system (14).

The POD basis vectors are computed using the method of snapshots. Consider the discrete state vector  $\mathbf{q}$  as the solution to one of the KdV equations (5), (10) or (14). The snapshot matrix is defined as

$$\mathcal{Q} := [\mathbf{q}^1, \dots, \mathbf{q}^{N_t}] \in \mathbb{R}^{N \times N_t},$$

where each column  $\mathbf{q}^k \in \mathbb{R}^N$  is the full discrete solution vector at discrete time instances  $t_k$ ,  $k = 1, \dots, N_t$ . We then expand the singular value decomposition (SVD) of the snapshot matrix

$$\mathcal{Q} = V \Sigma U^T,$$

where the columns of  $V \in \mathbb{R}^{N \times N_t}$  and  $U \in \mathbb{R}^{N_t \times N_t}$  are the left and right singular vectors of  $\mathcal{Q}$ , respectively, and  $\Sigma \in \mathbb{R}^{N_t \times N_t}$  is the diagonal matrix whose diagonal elements are the singular values  $\sigma_1 \geq \sigma_2 \geq \dots \geq \sigma_{N_t} \geq 0$ .

The  $n$ -POD basis matrix  $V_n \in \mathbb{R}^{N \times n}$  minimizes the least squares error of the snapshot reconstruction

$$\min_{V_n \in \mathbb{R}^{N \times n}} \|\mathcal{Q} - V_n V_n^T \mathcal{Q}\|_F^2 = \min_{V_n \in \mathbb{R}^{N \times n}} \sum_{k=1}^{N_t} \|\mathbf{q}^k - V_n V_n^T \mathbf{q}^k\|_2^2 = \sum_{k=n+1}^{N_t} \sigma_k^2,$$

where  $\|\cdot\|_2$  denotes the Euclidean 2-norm and  $\|\cdot\|_F$  denotes the Frobenius norm. The optimal solution of basis matrix  $V_n$  to this problem is given by the  $n$  left singular vectors of  $\mathcal{Q}$  corresponding to the  $n$  largest singular values.

The POD state approximation is  $\mathbf{q} \approx \hat{\mathbf{q}} = V_n \mathbf{q}_r$ , where  $\mathbf{q}_r \in \mathbb{R}^n$  is the reduced state vector. The POD reduced model is then defined by Galerkin projection

$$\frac{d}{dt} \mathbf{q}_r = V_n^T S \nabla_{\mathbf{q}} H(V_n \mathbf{q}_r). \quad (16)$$

Although the matrix  $S$  is a constant skew-symmetric matrix, the reduced-order system (16) based on Galerkin projection is not necessarily a skew-gradient system in general. The Hamiltonian structure can be preserved by inserting  $V_n V_n^T \in \mathbb{R}^{N \times N}$  between  $S$  and  $\nabla_{\mathbf{q}} H(V_n \mathbf{q}_r)$  in (16), which yields a small skew-gradient system [Karasözen and Uzunca(2018), Gong et al.(2017)Gong, Wang, and Wang, Miyatake(2019)]

$$\frac{d}{dt} \mathbf{q}_r = V_n^T S V_n V_n^T \nabla_{\mathbf{q}} H(V_n \mathbf{q}_r) = \hat{S} \nabla_{\mathbf{q}_r} \hat{H}(\mathbf{q}_r) \quad (17)$$

where  $\hat{S} := V_n^T S V_n$  and  $\hat{H}(\mathbf{q}_r) := H(V_n \mathbf{q}_r)$ .

The reduced cubic Hamiltonian  $\hat{H}$  is preserved by ROM, because the ROM (17) has the same skew-gradient form as the FOM (3). We remark that the periodic boundary conditions in the FOM are preserved in the ROMs [Sanderse(2020)].

The POD basis for the coupled PDEs, like the coupled KdV equation (10) are usually computed by stacking all  $\mathbf{u}$  and  $\mathbf{v}$  in one vector  $\mathbf{q} = (\mathbf{u}, \mathbf{v})^T$  and by taking the SVD of the snapshot data. But the resulting ROMs do not preserve the coupling topology structure of the FOM [Benner and Breiten(2015), Reis and Stykel(2007), Benner et al.(2020)Benner, Goyal, Kramer, Peherstorfer, and Willcox] and produce unstable reduced solutions. In order to maintain the coupling structure in ROMs, the POD basis vectors are computed separately for each the state vector  $\mathbf{u}$  and  $\mathbf{v}$ . Let  $Q_u, Q_v \in \mathbb{R}^{N \times N_t}$  be snapshot matrices for each state vector

$$Q_u = [\mathbf{u}^1, \dots, \mathbf{u}^{N_t}], \quad Q_v = [\mathbf{v}^1, \dots, \mathbf{v}^{N_t}].$$

The POD basis are computed taking the SVD of the snapshot matrix  $Q \in \mathbb{R}^{2N \times N_t}$

$$Q = \begin{pmatrix} Q_u \\ Q_v \end{pmatrix} = \begin{pmatrix} V_u & \\ & V_v \end{pmatrix} \begin{pmatrix} \Sigma_u & \\ & \Sigma_v \end{pmatrix} \begin{pmatrix} U_u^T & \\ & U_v^T \end{pmatrix}.$$

For PDEs like KdV equations with polynomial nonlinearities, ROMs do not require approximating the nonlinear terms through sampling hyper-reduction methods. Reduced-order operators can be precomputed in the offline stage. Projection of FOM onto the reduced space yields low-dimensional matrix operators that preserve the polynomial structure of the FOM. This is an advantage because the offline-online computation is separated in contrast to the hyper-reduction techniques like discrete empirical interpolation method, which may cause inaccuracies or instabilities in the ROM solutions in long term simulations. Recently, for PDEs with polynomial nonlinearities, the computationally efficient ROMs are constructed by the use of some tools from tensor theory and by matricizations of tensors [Benner et al.(2015)Benner, Gugercin, and Willcox, Benner et al.(2018)Benner, Goyal, and Gugercin, Benner and Goyal(2021)].

The dimension of the ROM (17) is supposed to be much smaller than the dimension of the FOM (15) ( $n \ll N$ ) for an efficient online computation of the ROM. But the computation of the quadratic terms of the reduced system still depends on the dimension of the FOM, with the computational cost of order  $\mathcal{O}(nN)$  [Ştefănescu et al.(2014)Ştefănescu, Sandu, and Navon]. This can be avoided by applying TPOD and exploiting the tensor matricization. TPOD separates the full spatial variables from the reduced time variables, allowing fast nonlinear term computations in the online stage. Using the Kronecker product  $\otimes$ , the FOM (15) can be written as the following linear-quadratic ODEs

$$\frac{d\mathbf{q}}{dt} = S \nabla_{\mathbf{q}} H(\mathbf{q}) = B_l \mathbf{q} + B_q W(\mathbf{q} \otimes \mathbf{q}), \quad (18)$$

where  $W \in \mathbb{R}^{N \times N^2}$  is the matricized tensor which satisfies the identity  $W(\mathbf{q} \otimes \mathbf{q}) = \mathbf{q} \odot \mathbf{q}$ . The linear-quadratic structure of the FOM (18) is preserved by the ROM [Benner et al.(2015)Benner, Gugercin, and Willcox]

$$\frac{d}{dt} \mathbf{q}_r = \widehat{B}_l \mathbf{q}_r + \widehat{B}_q \widehat{W}(\mathbf{q}_r \otimes \mathbf{q}_r), \quad (19)$$

where, for the single KdV equation (1),  $\widehat{B}_l$ ,  $\widehat{B}_q$  and  $\widehat{W}$  are given as

$$\widehat{B}_l = -\mu \widehat{S} V_n^T D_2 V_n, \quad \widehat{B}_q = -\frac{\alpha}{2} \widehat{S},$$

$$\widehat{S} = V_n^T D_1 V_n, \quad \widehat{W} = V_n^T W (V_n \otimes V_n).$$

The ROMs of the coupled KdV equation (8) and the Zakharov-Kuznetsov equation (11) can be defined similarly.

Using the TPOD, the computational cost of the reduced quadratic term in the ROM (19) becomes of order  $\mathcal{O}(n^3)$  [Ştefănescu et al.(2014)Ştefănescu, Sandu, and Navon], i.e., the offline and online computations are separated. On the other hand, TPOD requires the computation of the reduced tensor  $\widehat{W}$  in the offline stage, but the explicit computation of  $V_n \otimes V_n$  is inefficient because of the order  $\mathcal{O}(n^2 N^2)$  of the computational complexity. In order to avoid from this computational burden,  $V_n \otimes V_n$  is computed in an efficient way using  $W$  by  $\mu$ -mode matricizations of tensors [Benner and Breiten(2015)]. Recently algorithms are developed using tensor techniques to compute  $\widehat{W}$  by exploiting the particular structure of Kronecker product [Benner et al.(2018)Benner, Goyal, and Gugercin, Benner and Goyal(2021)], wherein,  $\widehat{W}$  is computed without explicitly forming  $W$  with the complexity of order  $\mathcal{O}(n^3 N)$  in contrast to the  $\mu$ -mode (matrix) computation. The reduced matrix  $\widehat{W}$  can be given in MATLAB notation as follows

$$\widehat{W} = V_n^T W (V_n \otimes V_n) = V_n^T \begin{pmatrix} V_n(1, :) \otimes V_n(1, :) \\ \vdots \\ V_n(N, :) \otimes V_n(N, :) \end{pmatrix}, \quad (20)$$

which utilizes the structure of  $W(V_n \otimes V_n)$ , without explicit construction of  $W$ . In [Benner et al.(2018)Benner, Goyal, and Gugercin, Benner and Goyal(2021)] the CUR matrix approximation [Mahoney and Drineas(2009)] of  $W(V_n \otimes V_n)$  is used to increase computational efficiency. Instead, here we make use of the "MULTIPROD" [Leva(2008)] to increase the computational efficiency of  $\widehat{W}$  in the offline stage. The MULTIPROD<sup>1</sup> handles multiple multiplications of the multi-dimensional arrays via virtual array expansion. It is a fast and memory efficient generalization for arrays of the MATLAB matrix multiplication operator. For any given two vectors  $\mathbf{a}$  and  $\mathbf{b}$ , the Kronecker product satisfies

$$(\text{vec}(\mathbf{b}\mathbf{a}^T))^T = (\mathbf{a} \otimes \mathbf{b})^T = \mathbf{a}^T \otimes \mathbf{b}^T,$$

where  $\text{vec}(\cdot)$  denotes the vectorization of a matrix. Using the above identity, the matrix  $C = W(V_n \otimes V_n) \in \mathbb{R}^{N \times n^2}$  can be constructed as

$$C(i, :) = (\text{vec}(V_n(i, :)^T V_n(i, :)))^T, \quad i \in \{1, 2, \dots, N\}. \quad (21)$$

Reshaping the matrix  $V_n \in \mathbb{R}^{N \times n}$  as  $\widetilde{V}_n \in \mathbb{R}^{N \times 1 \times n}$  and computing MULTIPROD of  $V_n$  and  $\widetilde{V}_n$  in the 2nd and 3rd dimensions, we obtain that

$$C = \text{MULTIPROD}(V_n, \widetilde{V}_n) \in \mathbb{R}^{N \times n \times n},$$

where the matrix  $C$  is recovered by reshaping the 3-dimensional array  $\mathcal{C}$  into a matrix of dimension  $N \times n^2$ . Without MULTIPROD, the computation of the matrix  $C$  in (21) requires  $N$  for loops within each iteration the matrix product of two matrices of sizes  $n \times 1$  and  $1 \times n$  are done. But, with the MULTIPROD, the matrix products are computed simultaneously in a single loop, and the matrix  $\widehat{W}$  in (20) can be efficiently computed [Karasözen et al.(2021)Karasözen, Yıldız, and Uzunca].

## 4 Numerical results

In this section, we demonstrate the performance of the structure-preserving ROM for the single KdV equation (1) with one and two solitons, the coupled symmetric KdV-KdV system (8), and the Zakharov-Kuznetsov equation (11). For all the problems, we prescribe periodic boundary conditions on the given spatial domain. In numerical test examples, we show only the preservation of the cubic integrals like the Hamiltonian (energy). Momentum as a quadratic invariant

<sup>1</sup><https://www.mathworks.com/matlabcentral/fileexchange/8773-multiple-matrix-multiplications-with-array-expansion-enabled>

is preserved by all the Runge Kutta methods of type (7) including the Kahan's method and the implicit-midpoint rule. Linear invariants like the mass are automatically preserved by the Runge-Kutta methods.

All the simulations are performed on a machine with Intel CoreTM i7 2.5 GHz 64 bit CPU, 16 GB RAM, Windows 10, using 64 bit MatLab R2014. The snapshot matrices resulting from the space-time discretization of the KdV equations are large, making SVD computations costly. Therefore, we use the randomized SVD (rSVD) algorithm [Halko et al.(2011)Halko, Martinsson, and Tropp] that performs SVD of small matrices, to efficiently generate a reduced basis.

In all examples, the number of (POD) modes is determined by the relative information content (RIC) formula

$$\mathcal{E}_{\text{ric}}(n) = \left( \frac{\sum_{k=1}^n \sigma_k^2}{\sum_{k=1}^{N_t} \sigma_k^2} \right) \times 100, \quad (22)$$

which can be thought as the percentage energy captured from the FOM. According to the RIC formula (22), we set the number of POD modes as the smallest positive integer  $n$  satisfying  $\mathcal{E}_{\text{ric}}(n) \geq 99.99$ .

The accuracy of the ROM solutions are measured by the time averaged relative  $L_2$ -errors

$$\|q - \hat{q}\|_{\text{rel}} = \frac{1}{N_t} \sum_{k=1}^{N_t} \frac{\|q^k - \hat{q}^k\|_{L^2(\Omega)}}{\|q^k\|_{L^2(\Omega)}}, \quad \|q^k\|_{L^2(\Omega)}^2 = \sum_{i=1}^N (q_i^k)^2 \Delta x \Delta y. \quad (23)$$

We measure the preservation of the reduced conserved quantities using the time-averaged absolute errors between the full and reduced quantities

$$\|E - \hat{E}\|_{\text{abs}} = \frac{1}{N_t} \sum_{k=1}^{N_t} |E(q^k) - \hat{E}(q_r^k)|, \quad E = H, I_1, \quad (24)$$

where  $\hat{E}(q_r^k) = E(V_n q_r^k)$  denotes the reduced quantity at the time  $t_k$ .

#### 4.1 Single KdV equation

We consider the one-dimensional single KdV equation (1) with  $\alpha = 6$ ,  $\mu = 1$  in the space-time domain  $[-10, 10] \times [0, 50]$ . For a positive parameter  $\beta$ , the initial condition is set to  $u(x, 0) = \beta \operatorname{sech}^2(\sqrt{\beta}x/2)$ , which leads to one soliton solutions. We set mesh size in space as  $\Delta x = 0.002$  and time step size is  $\Delta t = 0.005$ . The size of the snapshot matrix is  $Q \in \mathbb{R}^{10000 \times 10000}$ .

The singular values decay much slowly for larger values of  $\beta$  in Figure 1. Consequently, more modes are needed for accurate computation of the reduced solutions with increasing  $\beta$ . This behavior is characteristic for PDEs like the KdV equation exhibiting wave propagation phenomena, which require sufficiently large reduced spaces [Ohlberger and Rave(2016)].

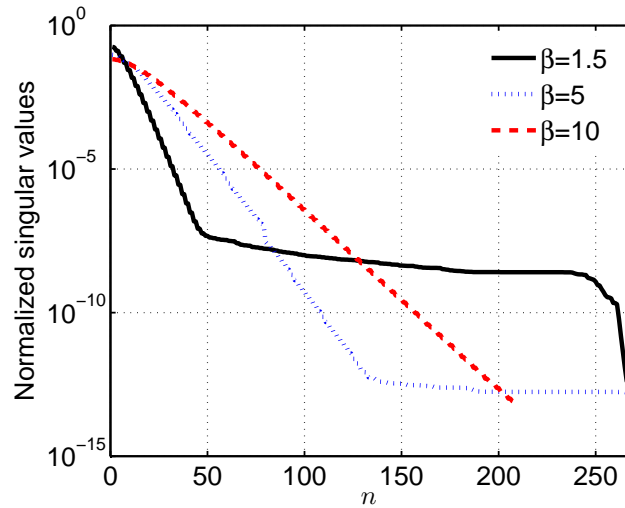


Figure 1: Singular values of the snapshot matrices by different values of  $\beta$ .

According to the RIC formula (22), the number of modes are taken as  $n = 30, 60, 90$  for  $\beta = 1.5, 5, 10$ , respectively. In Figure 2 the reduced approximations are plotted for  $\beta = 1.5, 5, 10$  for increasing number of modes. We observe that the relative  $L^2$ -errors (23) between the full and the reduced solutions decrease as the number of modes increases in Figure 2, bottom-right. The accuracy of the reduced solutions is improved as the number of modes is increased, upper and bottom left plots in Figure 2. They are visually not distinguishable<sup>2</sup> from the full solutions for the number of modes selected by the RIC formula and indicated by a circle in Figure 2, bottom-right.

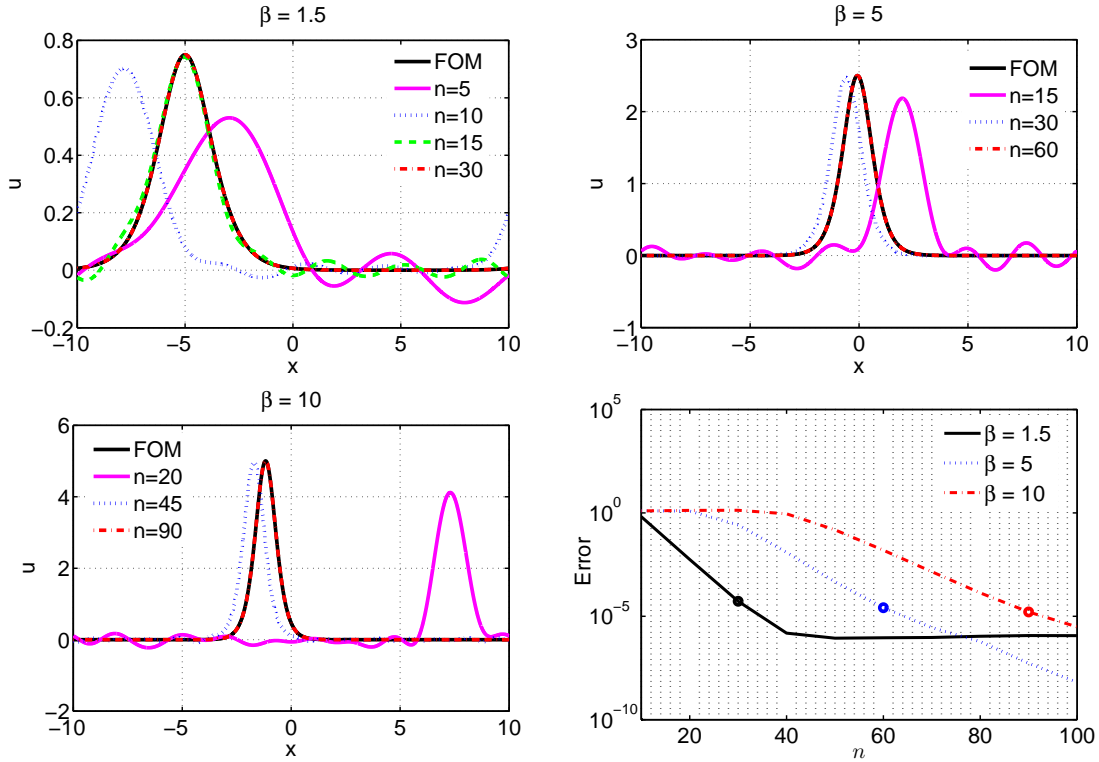


Figure 2: ROM profiles at  $T = 50$  and relative solution errors (23) between FOMs and ROMs for different number of modes  $n$  and for different values of  $\beta$ . The circles in the bottom-right plot indicate the number of modes calculated according to the RIC formula (22).

Figure 3 shows that the discrete cubic Hamiltonian (2) is preserved by the ROMs with high accuracy over time. The structure-preserving feature of the ROMs is well demonstrated by the solution errors (23) and errors of the conserved quantities (24) in Figure (4). The relative FOM-ROM errors of the solutions and the errors in the Hamiltonian  $H$  and the momentum  $I_1$  are decreasing for an increasing number of modes with small oscillations around  $n = 50 - 80$ .

<sup>2</sup>Animations are available as the supplementary material "Ex1\_sol.mp4".

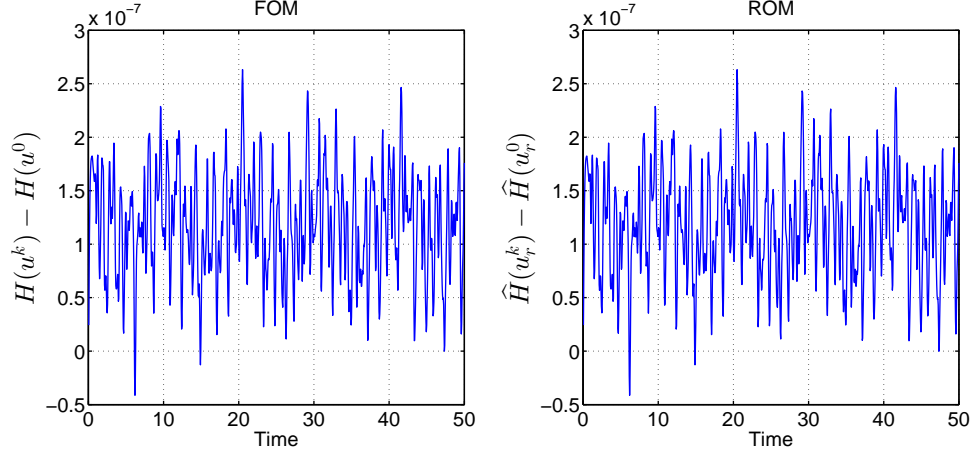


Figure 3: Time evolution of the full (left) and the reduced (right) Hamiltonian errors.

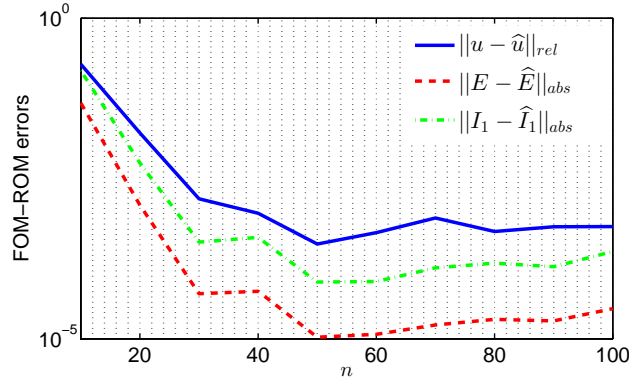


Figure 4: Relative solution errors and absolute errors of the conserved quantities.

In Table 1 the relative solution errors (23), conservation errors (24) of the Hamiltonian and the momentum are given for  $\beta = 1.5, 5, 10$ . With increasing values of  $\beta$ , more modes are needed for accurate reduced solutions and for the conservation of the Hamiltonian and the momentum.

Table 1: Hamiltonian, momentum and solution errors between the FOMs and ROMs

| # modes | $\beta = 1.5$           |                         |                             | $\beta = 5$             |                         |                             | $\beta = 10$            |                         |                             |
|---------|-------------------------|-------------------------|-----------------------------|-------------------------|-------------------------|-----------------------------|-------------------------|-------------------------|-----------------------------|
|         | $\ u - \hat{u}\ _{rel}$ | $\ H - \hat{H}\ _{abs}$ | $\ I_1 - \hat{I}_1\ _{abs}$ | $\ u - \hat{u}\ _{rel}$ | $\ H - \hat{H}\ _{abs}$ | $\ I_1 - \hat{I}_1\ _{abs}$ | $\ u - \hat{u}\ _{rel}$ | $\ H - \hat{H}\ _{abs}$ | $\ I_1 - \hat{I}_1\ _{abs}$ |
| 10      | 6.52e-01                | 1.34e-02                | 5.06e-03                    | 1.26e+00                | 2.76e+00                | 6.06e-01                    | 1.24e+00                | 2.98e+01                | 4.35e+00                    |
| 20      | 5.53e-03                | 3.42e-05                | 4.84e-06                    | 1.22e+00                | 2.04e-01                | 2.12e-02                    | 1.31e+00                | 6.37e+00                | 4.90e-01                    |
| 30      | 5.28e-05                | 4.43e-08                | 2.96e-09                    | 2.60e-01                | 8.74e-03                | 4.69e-04                    | 1.33e+00                | 8.51e-01                | 3.55e-02                    |
| 40      | 1.52e-06                | 7.16e-11                | 1.04e-10                    | 1.23e-02                | 2.79e-04                | 7.54e-06                    | 8.94e-01                | 1.03e-01                | 1.45e-03                    |
| 50      | 8.68e-07                | 1.02e-10                | 1.07e-10                    | 4.64e-04                | 7.33e-06                | 6.00e-08                    | 1.51e-01                | 8.10e-03                | 6.39e-05                    |
| 60      | 9.13e-07                | 9.71e-11                | 1.07e-10                    | 2.57e-05                | 1.69e-07                | 1.29e-09                    | 1.56e-02                | 6.05e-04                | 2.09e-05                    |
| 70      | 9.44e-07                | 9.42e-11                | 1.08e-10                    | 2.83e-06                | 3.53e-09                | 8.49e-11                    | 1.42e-03                | 4.09e-05                | 2.88e-06                    |
| 80      | 1.08e-06                | 6.73e-11                | 1.09e-10                    | 5.90e-07                | 2.41e-10                | 2.25e-12                    | 1.35e-04                | 2.38e-06                | 3.39e-07                    |
| 90      | 1.17e-06                | 5.86e-11                | 1.09e-10                    | 5.33e-08                | 6.41e-12                | 3.23e-12                    | 1.61e-05                | 1.53e-07                | 2.66e-08                    |
| 100     | 1.15e-06                | 5.84e-11                | 1.09e-10                    | 6.42e-09                | 7.75e-12                | 3.12e-12                    | 3.06e-06                | 8.86e-09                | 2.18e-09                    |

## 4.2 Two soliton interaction

As the second test problem, we consider for  $\alpha = 1$  and  $\mu = 1$  the one-dimensional two soliton KdV equation (1) with the exact solution [Brugnano et al.(2019)Brugnano, Gurioli, and Sun, Bo et al.(2020)Bo, Wang, and Cai,

Liu and Yi(2016)]

$$u_e(x, t) = 12 \frac{k_1^2 e^{\xi_1} + k_2^2 e^{\xi_2} + 2(k_2 - k_1) e^{\xi_1 + \xi_2} + \rho^2 (k_2^2 e^{\xi_1} + k_1^2 e^{\xi_2} e^{\xi_1 + \xi_2})}{(1 + e^{\xi_1} + e^{\xi_2} + \rho^2 e^{\xi_1 + \xi_2})^2}. \quad (25)$$

The parameters are

$$\begin{aligned} k_1 &= 0.4, & k_2 &= 0.6, & \rho &= (k_1 - k_2)/(k_1 + k_2) = -0.2, \\ \xi_1 &= k_1 x - k_1^3 t + 4, & \xi_2 &= k_2 x - k_2^3 t + 15. \end{aligned}$$

We take the space domain  $\Omega = [-40, 40]$ , and set the final time  $T = 120$  as in [Bo et al.(2020)Bo, Wang, and Cai, Liu and Yi(2016)].

To determine the experimental orders of convergence (EOC) of the high-fidelity solutions, the mesh size is uniformly refined by a factor of two in both space and time dimensions. The EOC is calculated as

$$\text{order} = \frac{1}{\log 2} \log \left( \frac{\text{error}(\Delta x, \Delta t)}{\text{error}(\Delta x/2, \Delta t/2)} \right), \quad (26)$$

where  $\text{error}(\Delta x, \Delta t)$  denotes the relative  $L^2$ -error between the exact solution (25) and the numerical solution at the final time, computed with the spatial and temporal mesh sizes  $\Delta x$  and  $\Delta t$ , respectively. The calculated errors and their EOC are summarized in Table 2. They confirm the expected second order rate of convergence of the centred finite difference scheme and Kahan's method.

Table 2: Relative  $L^2$ -errors between the exact and FOM solutions, and experimental order of convergence

|            |          |          |          |          |          |          |
|------------|----------|----------|----------|----------|----------|----------|
| $\Delta t$ | 0.5      | 0.25     | 0.125    | 0.0625   | 0.03125  | 0.016625 |
| $\Delta x$ | 4        | 2        | 1        | 0.5      | 0.25     | 0.125    |
| Error      | 2.42e-00 | 9.68e-01 | 2.35e-01 | 5.72e-02 | 1.42e-02 | 3.55e-03 |
| Order      | -        | 1.3226   | 2.0445   | 2.0359   | 2.0124   | 1.9970   |

We take the spatial mesh size as  $\Delta x = 0.125$  and the time step  $\Delta t = 0.05$ , that leads to the snapshot matrix  $Q \in \mathbb{R}^{640 \times 2400}$ . The singular value spectrum in Figure 5 behaves similar to the single KdV equation with  $\beta = 1.5$ . 30 modes are sufficient to capture the behavior of the FOM soliton waves according to the RIC formula (22).

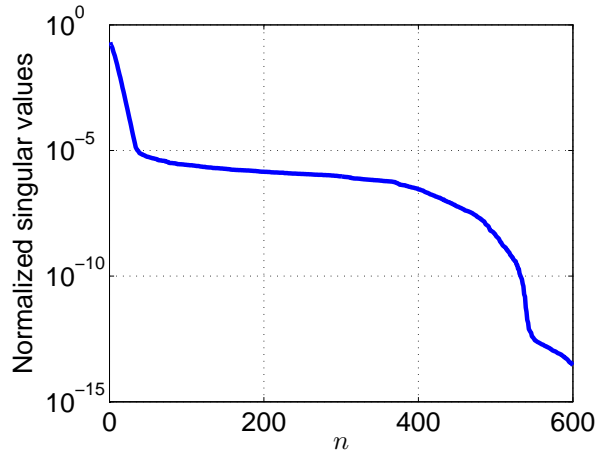


Figure 5: Singular values of the snapshot matrix.

In Figure 6, the two soliton waves<sup>3</sup> with a taller and a lower one, moving to the right and collide at  $t = 80$ , continue moving away from each other until the final time  $t = 120$  in Figure 6 as in [Bo et al.(2020)Bo, Wang, and Cai, Liu and Yi(2016)]. The ROM profiles in Figure 6 at the collision time and at the final time show that with an increasing

<sup>3</sup>Animations are available as the supplementary material "Ex2\_sol.mp4".

number of modes they approximate the full solutions more closely and finally catch them for  $n = 30$  according to the RIC formula (22).

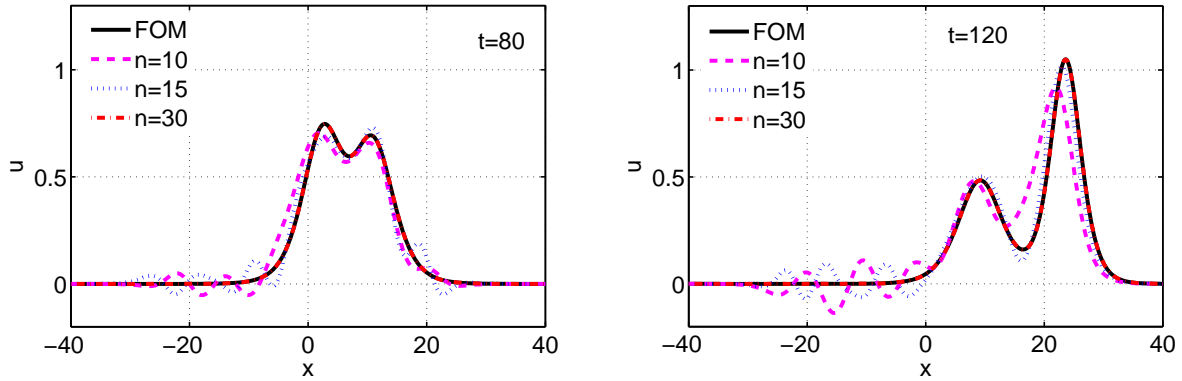


Figure 6: FOM and ROM profiles at collision time  $t = 80$  and at final time  $t = 120$  for different number of modes.

Furthermore, we show the propagation of the relative  $L^2$ -errors  $\|u(x, t) - u_e(x, t)\|_{L^2(\Omega)} / \|u_e(x, t)\|_{L^2(\Omega)}$  between the exact solution  $u_e(x, t)$  and FOM/ROM solutions in Figure 7. The circles indicate that the maximum of the errors occur at the final time. In the reduced order modelling framework, the reduced solutions are expected to behave similar to the full solutions, since the reduced space is constructed from the FOM. Correspondingly, the errors of the reduced solutions in Figure 7 show similar behavior as the full solution errors. This also indicates that the location and the shape of the full soliton waves are well-captured by the ROM solutions with increasing number of modes. The almost linear error growth rate in time in Figure 7 is characteristic for Hamiltonian preserving and for the geometric integrators [Hairer et al.(2010)Hairer, Lubich, and Wanner] including Kahan's method.

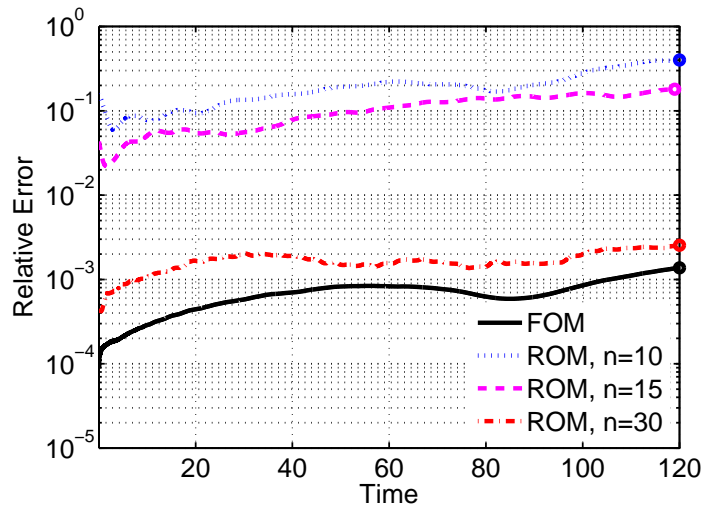


Figure 7: Error propagation of relative  $L^2$ -errors between exact and FOM/ROM solutions.

In Figure 8, the Hamiltonian errors do not show any drift, they are preserved not with a high accuracy as in the single soliton example, which might be due to the interaction of the solitons.

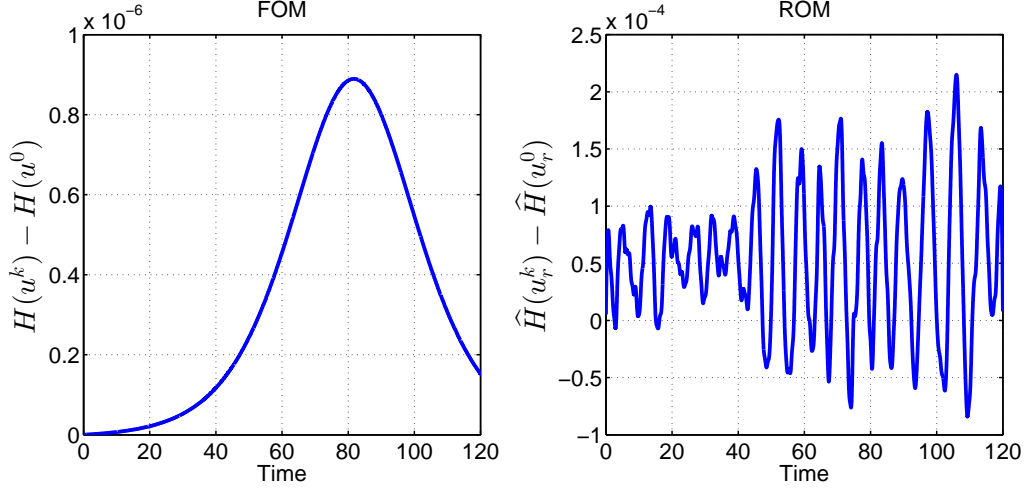


Figure 8: Time evolution of the full (left) and the reduced (right) Hamiltonian errors.

### 4.3 Coupled KdV equation

Symmetric KdV-KdV equation under periodic boundary conditions possesses solitary pulse solutions decaying symmetrically to oscillations of small, constant amplitude [Bona et al.(2007)Bona, Dougalis, and Mitsotakis, Bona et al.(2008)Bona, Dougalis, and Mitsotakis]. The solutions are in the form of traveling waves with main pulses like the classical solitary waves and dispersive oscillations following the main pulses. For the coupled KdV-KdV equation (8), we take the initial conditions as in [Karasözen and Şimşek(2012), Bona et al.(2008)Bona, Dougalis, and Mitsotakis]

$$u(x, 0) = 0, \quad v(x, 0) = 0.3e^{-(x+100)^2/25}.$$

We set the space-time domain as  $[-150, 150] \times [0, 50]$ , and the mesh sizes are  $\Delta x = 0.1$  and  $\Delta t = 0.05$ . The size of the snapshot matrix is  $Q \in \mathbb{R}^{3000 \times 1000}$ .

In Figure 9 the singular values decay monotonically without reaching a plateau as for the single KdV equation with  $\beta = 10$  in Figure 1. The number of modes is determined again by the RIC formula (22) as  $n = 30$  and  $n = 28$  for  $u$  and  $v$  components, respectively. The reduced and full solutions<sup>4</sup> in Figure 10 are visually indistinguishable, and again the discrete Hamiltonian(9) is preserved accurately by the ROMs in Figure 11.

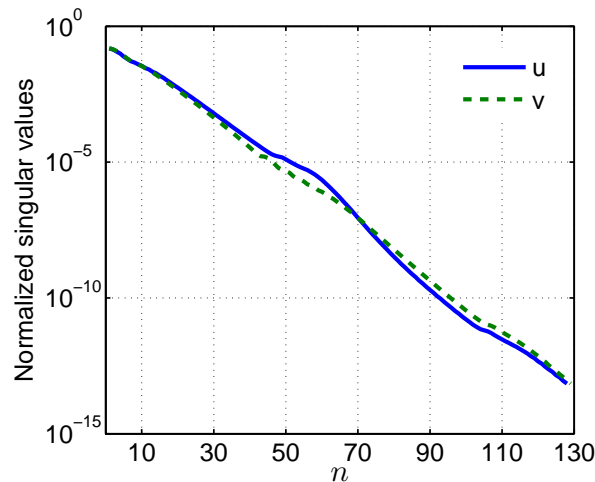


Figure 9: Singular values of the snapshot matrices.

<sup>4</sup>Animations are available as the supplementary material "Ex3\_sol.mp4".

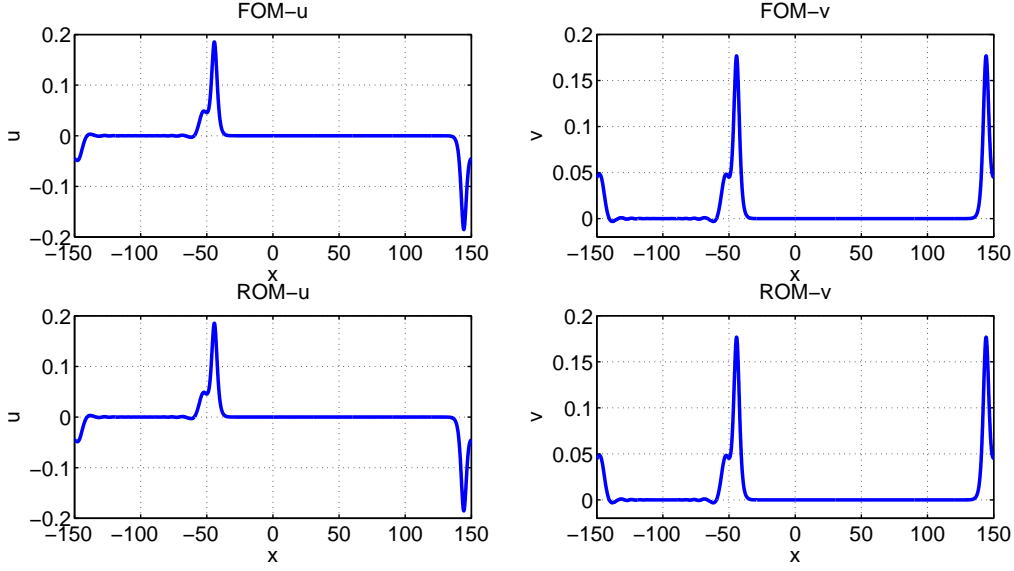
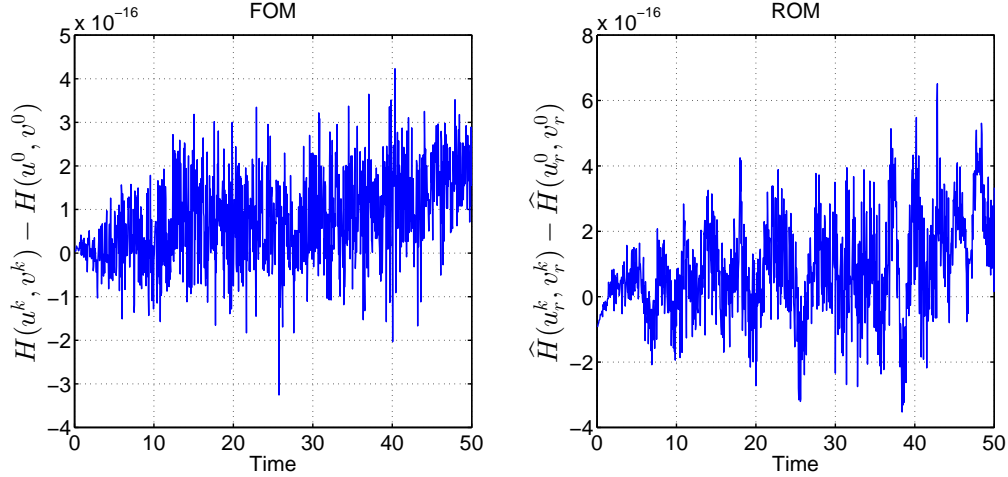
Figure 10: FOM and ROM solutions at  $T = 50$ .

Figure 11: Time evolution of the full (left) and the reduced (right) Hamiltonian errors.

#### 4.4 Zakharov-Kuznetsov equation

We simulate cylindrically symmetric waves of the Zakharov-Kuznetsov equation (11), that are called as bell-shaped pulses [Chen et al.(2011)Chen, Song, and Zhu, Iwasaki et al.(1990)Iwasaki, Toh, and Kawahara, Nishiyama et al.(2012)Nishiyama, Noi, and Oharu] with  $\alpha = 6$ ,  $\mu = 1$ . The initial condition for two pulses is given by

$$u(x, y, 0) = \sum_{j=1}^2 \frac{c_j}{3} \sum_{m=1}^{10} a_{2m} \left( \cos \left( 2m \arccot \left( \frac{\sqrt{c_j}}{2} r_j \right) \right) - 1 \right),$$

where  $c_1$  and  $c_2$  are the velocities of the solitary wave solutions, and  $r_i$  is defined by  $r_i^2 = (x - x_i)^2 + (y - y_i)^2$ ,  $i = 1, 2$ . The points  $(x_i, y_i)$  are the location of the peak of  $u$ . The coefficients  $a_{2m}$  are given in [Nishiyama et al.(2012)Nishiyama, Noi, and Oharu].

Numerical solutions are computed in the rectangular space domain  $[0, 32] \times [0, 32]$  and in the time interval  $[0, 5]$  using a fine discretization both in space and time,  $\Delta x = \Delta y = 0.2286$ ,  $\Delta t = 0.01$ , to simulate the waves accurately as in

[Chen et al.(2011)Chen, Song, and Zhu, Nishiyama et al.(2012)Nishiyama, Noi, and Oharu]. The snapshot matrix is of size  $19600 \times 500$ .

The decay of the singular values in Figure 12 shows similar behavior as for the single KdV equations in the Figure 1 and in the Figure 9. The number of retained POD modes is  $n = 50$  according to the RIC formula.

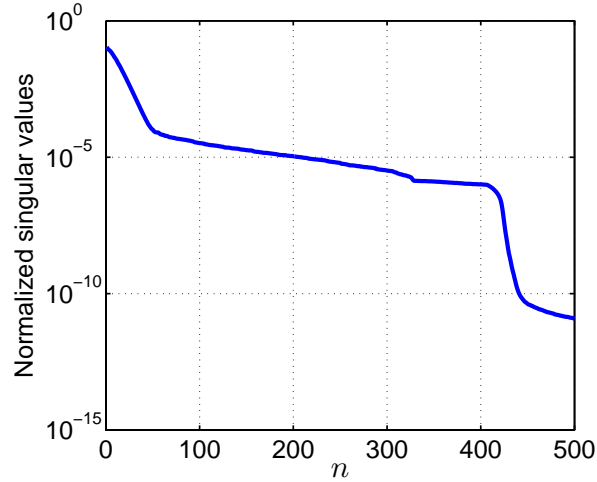


Figure 12: Singular values of the snapshot matrix.

In Figure 13, the initial profile, the FOM and ROM profiles<sup>5</sup> at the final time  $T = 5$  are presented. Two dissimilar pulse wave solutions to the Zakharov-Kuznetsov equation at the initial time, evolving in time where the wave structure changes after the collision, where the stronger pulse becomes further stronger and the weaker one gets further weaker after the collision as in Figure 13 by both FOM and ROM. The discrete Hamiltonian (13) is well preserved by the ROM in Figure 14, even though both Hamiltonian errors are not so small as for the one-dimensional single and coupled KdV equations. However, from the geometric integration point of view, the Hamiltonian should not drift with time, which is the case for both the full and reduced discrete Hamiltonian in Figure 14.

<sup>5</sup>Animations are available as the supplementary materials "Ex4\_Contour.mp4" and "Ex4\_Piece.mp4".

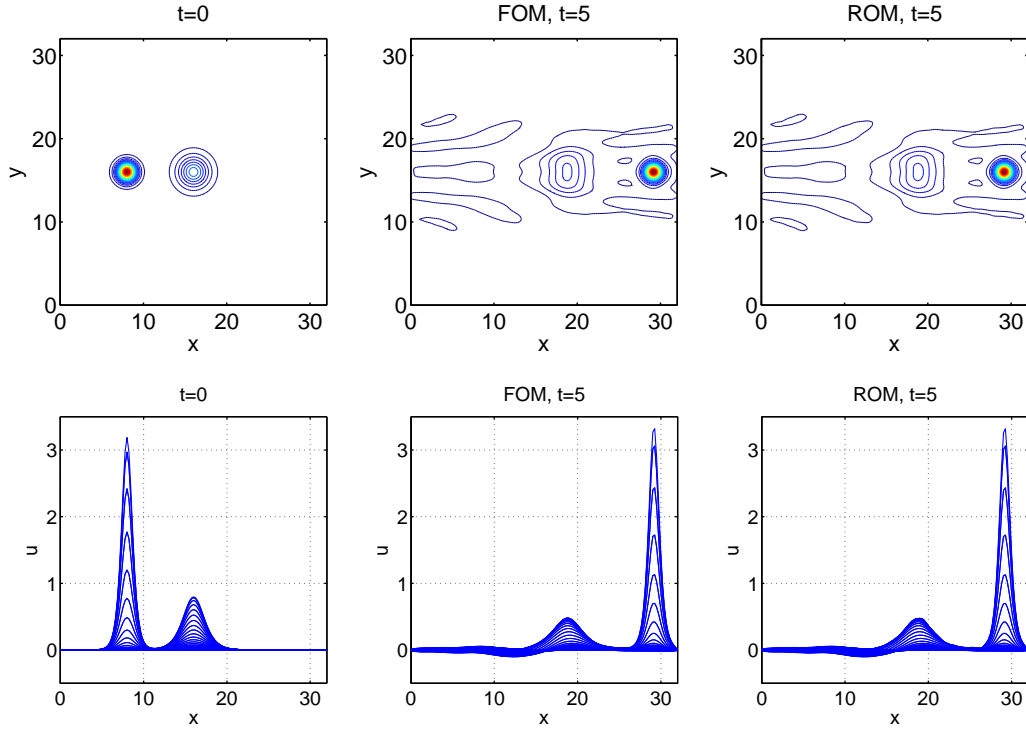
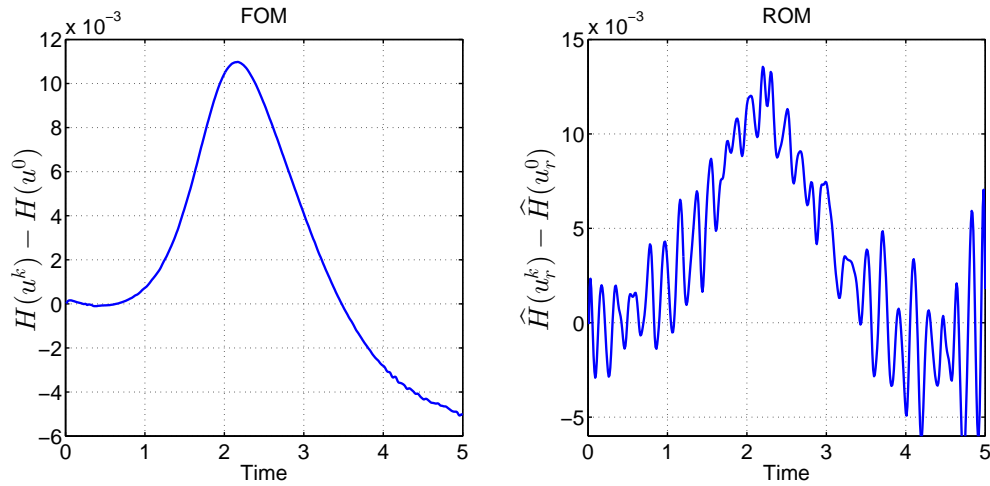
Figure 13: Initial profiles, FOM and ROM profiles at  $t = 5$ , from left to right.

Figure 14: Time evolution of the full (left) and the reduced (right) Hamiltonian errors.

#### 4.5 Computational efficiency

In Table 3, we present the computational efficiency of the POD and TPOD. The computational cost of the FOM consists of the time required to solve the full solutions, i.e., the creation of snapshots. The computational cost in the offline phase consists of the time required to compute the singular values and singular vectors (POD basis), and the calculation of precomputed matrices. The computational cost in the online phase consists of the time required to solve the reduced system. In order to measure that to what extent the ROM accelerates the solution process, the speed-up factors are calculated as the ratio of wall-clock time required to solve the FOMs over the wall-clock time required to solve the ROMs in the online phase. We see that the TPOD approach utilizing MULTIPROD is much faster than the

POD, where speed-up factors are given in parenthesis in Table 3. The efficiency of the TPOD over the POD is much pronounced for the KdV equation with one soliton wave and  $\beta = 1.5$ , and for the Zakharov-Kuznetsov equation, because of larger spatial discretization of the FOMs. In addition, for the single KdV equation with one soliton, the computational efficiency deteriorates with the increasing values of  $\beta$  and the number of modes.

Table 3: Wall clock times (in seconds) and speed-up factors (in bold parenthesis)

| System                        | $n$    | FOM    | POD     |                       | TPOD    |                       |
|-------------------------------|--------|--------|---------|-----------------------|---------|-----------------------|
|                               |        |        | Offline | Online                | Offline | Online                |
| One soliton ( $\beta = 1.5$ ) | 30     | 178.06 | 5.28    | 62.66 ( <b>2.8</b> )  | 5.67    | 5.55 ( <b>32.1</b> )  |
| One soliton ( $\beta = 5$ )   | 60     | 185.62 | 7.49    | 80.70 ( <b>2.3</b> )  | 8.11    | 46.30 ( <b>4.0</b> )  |
| One soliton ( $\beta = 10$ )  | 90     | 188.81 | 8.25    | 157.34 ( <b>1.2</b> ) | 9.79    | 124.40 ( <b>1.5</b> ) |
| Two solitons                  | 30     | 7.26   | 1.70    | 2.94 ( <b>2.5</b> )   | 1.71    | 2.34 ( <b>3.1</b> )   |
| Coupled KdV                   | 30, 28 | 17.85  | 1.96    | 2.97 ( <b>6.0</b> )   | 2.01    | 1.79 ( <b>9.9</b> )   |
| Zakharov-Kuznetsov equation   | 50     | 61.15  | 3.33    | 9.25 ( <b>6.6</b> )   | 3.67    | 0.90 ( <b>68.1</b> )  |

## 5 Conclusions

We have constructed computationally efficient and accurate ROMs for KdV equations by exploiting the non-canonical Hamiltonian structure. It is difficult to capture the wave dynamics of PDEs like the KdV equation with a few POD modes. Therefore, in all numerical test problems, the number of the POD modes is relatively large to achieve accurate reduced solutions and to preserve the conserved quantities. Using TPOD and exploiting the quadratic structure of the KdV equations, the online computational time of ROMs is reduced further. In a future study, we plan to extend the results of this paper to the parametrized problems using the POD/TPOD-greedy approach in time and in parametric space.

**Acknowledgements:** The authors thank for the constructive comments of the referees, which helped much to improve the paper.

## References

- [Benner et al.(2017)Benner, Cohen, Ohlberger, and Willcox] P. Benner, A. Cohen, M. Ohlberger, K. Willcox (Eds.), Model reduction and approximation, volume 15 of *Computational Science & Engineering*, Society for Industrial and Applied Mathematics (SIAM), Philadelphia, PA, 2017. doi:doi:10.1137/1.9781611974829.
- [Quarteroni and Rozza(2014)] A. Quarteroni, G. Rozza (Eds.), Reduced order methods for modeling and computational reduction, volume 9 of *MS&A. Modeling, Simulation and Applications*, Springer, Cham, 2014. doi:doi:10.1007/978-3-319-02090-7, selected papers from the workshop “Reduced Basis, POD and Reduced Order Methods for Model and Computational Reduction: Towards Real-Time Computing and Visualization?” held at Ecole Polytechnique Fédérale de Lausanne, Lausanne, May 14–16, 2012.
- [Hesthaven et al.(2016)Hesthaven, Rozza, and Stamm] J. S. Hesthaven, G. Rozza, B. Stamm, Certified reduced basis methods for parametrized partial differential equations, SpringerBriefs in Mathematics, Springer, Cham; BCAM Basque Center for Applied Mathematics, Bilbao, 2016. doi:doi:10.1007/978-3-319-22470-1, bCAM Springer-Briefs.
- [Berkooz et al.(1993)Berkooz, Holmes, and Lumley] G. Berkooz, P. Holmes, J. L. Lumley, The proper orthogonal decomposition in the analysis of turbulent flows, *Annual Review of Fluid Mechanics* 25 (1993) 539–575. doi:doi:10.1146/annurev.fl.25.010193.002543.
- [Sirovich(1987)] L. Sirovich, Turbulence and the dynamics of coherent structures. III. Dynamics and scaling, *Quart. Appl. Math.* 45 (1987) 583–590. doi:doi:10.1090/qam/910464.
- [Hairer et al.(2016)Hairer, Lubich, and Wanner] E. Hairer, C. Lubich, G. Wanner, Geometric numerical integration: Structure-preserving algorithms for ordinary differential equations, Springer Series in Computational Mathematics, Springer, Heidelberg, 2016. doi:doi:10.1007/978-3-662-05018-7.
- [Carlberg et al.(2013)Carlberg, Farhat, Cortial, and Amsallem] K. Carlberg, C. Farhat, J. Cortial, D. Amsallem, The GNAT method for nonlinear model reduction: effective implementation and application to compu-

- tational fluid dynamics and turbulent flows, *Journal of Computational Physics* 242 (2013) 623 – 647. doi:doi:10.1016/j.jcp.2013.02.028.
- [Chaturantabut et al.(2016)Chaturantabut, Beattie, and Gugercin] S. Chaturantabut, C. Beattie, S. Gugercin, Structure-preserving model reduction for nonlinear port-Hamiltonian systems, *SIAM Journal on Scientific Computing* 38 (2016) B837–B865. doi:doi:10.1137/15M1055085.
- [Afkham and Hesthaven(2019)] B. M. Afkham, J. S. Hesthaven, Structure-preserving model-reduction of dissipative Hamiltonian systems, *J. Sci. Comput.* 81 (2019) 3–21. doi:doi:10.1007/s10915-018-0653-6.
- [Afkham and Hesthaven(2017)] B. M. Afkham, J. S. Hesthaven, Structure preserving model reduction of parametric Hamiltonian systems, *SIAM J. Sci. Comput.* 39 (2017) A2616–A2644. doi:doi:10.1137/17M1111991.
- [Buchfink et al.(2019)Buchfink, Bhatt, and Haasdonk] P. Buchfink, A. Bhatt, B. Haasdonk, Symplectic model order reduction with non-orthonormal bases, *Mathematical and Computational Applications* 24 (2019). doi:doi:10.3390/mca24020043.
- [Hesthaven and Pagliantini(2020)] J. S. Hesthaven, C. Pagliantini, Structure-preserving reduced basis methods for Hamiltonian systems with a state-dependent Poisson structure, *Mathematics of Computation* (2020). URL: <http://infoscience.epfl.ch/record/256097>.
- [Peng and Mohseni(2016)] L. Peng, K. Mohseni, Symplectic model reduction of Hamiltonian systems, *SIAM Journal on Scientific Computing* 38 (2016) A1–A27. doi:doi:10.1137/140978922.
- [Karasözen and Uzunca(2018)] B. Karasözen, M. Uzunca, Energy preserving model order reduction of the nonlinear Schrödinger equation, *Advances in Computational Mathematics* 44 (2018) 1769–1796. doi:doi:10.1007/s10444-018-9593-9.
- [Gong et al.(2017)Gong, Wang, and Wang] Y. Gong, Q. Wang, Z. Wang, Structure-preserving Galerkin POD reduced-order modeling of Hamiltonian systems, *Computer Methods in Applied Mechanics and Engineering* 315 (2017) 780 – 798. doi:doi:10.1016/j.cma.2016.11.016.
- [Miyatake(2019)] Y. Miyatake, Structure-preserving model reduction for dynamical systems with a first integral, *Japan Journal of Industrial and Applied Mathematics* 36 (2019) 1021–1037. doi:doi:10.1007/s13160-019-00378-y.
- [Hesthaven and Pagliantini(2018)] J. S. Hesthaven, C. Pagliantini, Structure-Preserving Reduced Basis Methods for Hamiltonian Systems with a Nonlinear Poisson Structure, Technical Report, EPFL scientific publications, 2018. URL: <http://infoscience.epfl.ch/record/256097>.
- [Gerbeau and Lombardi(2014)] J.-F. Gerbeau, D. Lombardi, Approximated Lax pairs for the reduced order integration of nonlinear evolution equations, *Journal of Computational Physics* 265 (2014) 246 – 269. doi:doi:10.1016/j.jcp.2014.01.047.
- [Ehrlacher et al.(2020)Ehrlacher, Lombardi, Mula, and Vialárd] V. Ehrlacher, D. Lombardi, O. Mula, F. X. Vialárd, Nonlinear model reduction on metric spaces. application to one-dimensional conservative PDEs in Wasserstein spaces, *ESAIM: Mathematical Modelling and Numerical Analysis* (2020). doi:doi:10.1051/m2an/2020013.
- [Barrault et al.(2004)Barrault, Maday, Nguyen, and Patera] M. Barrault, Y. Maday, N. C. Nguyen, A. T. Patera, An ‘empirical interpolation’ method: application to efficient reduced-basis discretization of partial differential equations, *C. R. Math. Acad. Sci. Paris* 339 (2004) 667–672. doi:doi:10.1016/j.crma.2004.08.006.
- [Chaturantabut and Sorensen(2010)] S. Chaturantabut, D. C. Sorensen, Nonlinear model reduction via discrete empirical interpolation, *SIAM Journal on Scientific Computing* 32 (2010) 2737–2764. doi:doi:10.1137/090766498.
- [Celledoni et al.(2012)Celledoni, Grimm, McLachlan, McLaren, O’Neale, Owren, and Quispel] E. Celledoni, V. Grimm, R. I. McLachlan, D. I. McLaren, D. O’Neale, B. Owren, G. R. W. Quispel, Preserving energy resp. dissipation in numerical pdes using the ‘Average Vector Field’ method, *Journal of Computational Physics* 231 (2012) 6770 – 6789. doi:doi:10.1016/j.jcp.2012.06.022.
- [Kahan and Li(1997)] W. Kahan, R.-C. Li, Unconventional schemes for a class of ordinary differential equations with applications to the Korteweg-de Vries equation, *Journal of Computational Physics* 134 (1997) 316 – 331. doi:doi:10.1006/jcph.1997.5710.
- [Celledoni et al.(2013)Celledoni, McLachlan, Owren, and Quispel] E. Celledoni, R. I. McLachlan, B. Owren, G. R. W. Quispel, Geometric properties of Kahan’s method, *Journal of Physics A: Mathematical and Theoretical* 46 (2013) 025201. doi:doi:10.1088/1751-8113/46/2/025201.
- [Celledoni et al.(2015)Celledoni, McLachlan, McLaren, Owren, and Quispel] E. Celledoni, R. I. McLachlan, D. I. McLaren, B. Owren, G. R. W. Quispel, Discretization of polynomial vector fields by polarization, *Proceedings of the Royal Society of London A: Mathematical, Physical and Engineering Sciences* 471 (2015). doi:doi:10.1098/rspa.2015.0390.

- [Benner et al.(2018)Benner, Goyal, and Gugercin] P. Benner, P. Goyal, S. Gugercin,  $\mathcal{H}_2$ -quasi-optimal model order reduction for quadratic-bilinear control systems, *SIAM Journal on Matrix Analysis and Applications* 39 (2018) 983–1032. doi:doi:10.1137/16M1098280.
- [Benner and Breiten(2015)] P. Benner, T. Breiten, Two-sided projection methods for nonlinear model order reduction, *SIAM Journal on Scientific Computing* 37 (2015) B239–B260. doi:doi:10.1137/14097255X.
- [Kramer and Willcox(2019)] B. Kramer, K. E. Willcox, Nonlinear model order reduction via lifting transformations and proper orthogonal decomposition, *AIAA Journal* 57 (2019) 2297–2307. doi:doi:10.2514/1.J057791.
- [Benner and Goyal(2021)] P. Benner, P. Goyal, Interpolation-based model order reduction for polynomial systems, *SIAM Journal on Scientific Computing* 43 (2021) A84–A108. doi:doi:10.1137/19M1259171.
- [Leva(2008)] P. D. Leva, MULTIPROD TOOLBOX, multiple matrix multiplications, with array expansion enabled, Technical Report, University of Rome Foro Italico, Rome, 2008.
- [Nutku and Oğuz(1990)] Y. Nutku, O. Oğuz, Bi-Hamiltonian structure of a pair of coupled KdV equations, *Nuovo Cimento B* (11) 105 (1990). doi:doi:10.1007/BF02742693.
- [Karasözen and Şimşek(2013)] B. Karasözen, G. Şimşek, Energy preserving integration of bi-Hamiltonian partial differential equations, *Appl. Math. Lett.* 26 (2013) 1125–1133. doi:doi:10.1016/j.aml.2013.06.005.
- [Ascher and McLachlan(2005)] U. M. Ascher, R. I. McLachlan, On symplectic and multisymplectic schemes for the KdV equation, *Journal of Scientific Computing* 25 (2005) 83–104. doi:doi:10.1007/s10915-004-4634-6.
- [Chen et al.(2011)Chen, Song, and Zhu] Y. Chen, S. Song, H. Zhu, The multi-symplectic Fourier pseudospectral method for solving two-dimensional Hamiltonian PDEs, *Journal of Computational and Applied Mathematics* 236 (2011) 1354 – 1369. doi:doi:10.1016/j.cam.2011.08.023.
- [Bridges and Reich(2001)] T. J. Bridges, S. Reich, Multi-symplectic spectral discretizations for the Zakharov-Kuznetsov and shallow water equations, *Physica D: Nonlinear Phenomena* 152-153 (2001) 491 – 504. doi:doi:10.1016/S0167-2789(01)00188-9.
- [Eidnes and Li(2020)] S. Eidnes, L. Li, Linearly implicit local and global energy-preserving methods for PDEs with a cubic Hamiltonian, *SIAM Journal on Scientific Computing* 42 (2020) A2865–A2888. doi:doi:10.1137/19M1272688.
- [Karasözen and Şimşek(2012)] B. Karasözen, G. Şimşek, Energy preserving integration of KdV-KdV systems, *TWMS J. Appl. Eng. Math.* 2 (2012) 219–227. URL: <http://jaem.isikun.edu.tr/web/images/articles/vol.2.no.2/08.pdf>.
- [Sanz-Serna(1994)] J. Sanz-Serna, An unconventional symplectic integrator of W. Kahan, *Applied Numerical Mathematics* 16 (1994) 245 – 250. doi:doi:10.1016/0168-9274(94)00030-1.
- [Matsuo and Furihata(2001)] T. Matsuo, D. Furihata, Dissipative or conservative finite-difference schemes for complex-valued nonlinear partial differential equations, *Journal of Computational Physics* 171 (2001) 425 – 447. doi:doi:10.1006/jcph.2001.6775.
- [Dahlby and Owren(2011)] M. Dahlby, B. Owren, A general framework for deriving integral preserving numerical methods for PDEs, *SIAM Journal on Scientific Computing* 33 (2011) 2318–2340. doi:doi:10.1137/100810174.
- [Eidnes et al.(2019)Eidnes, Li, and Sato] S. Eidnes, L. Li, S. Sato, Linearly implicit structure-preserving schemes for Hamiltonian systems, *Journal of Computational and Applied Mathematics* (2019) 112489. doi:doi:10.1016/j.cam.2019.112489.
- [Hardin(1973)] R. H. Hardin, Application of the split-step fourier method to the numerical solution of nonlinear and variable coefficient wave equations, *Siam Review* 15 (1973) 423.
- [Bona et al.(2007)Bona, Dougalis, and Mitsotakis] J. Bona, V. Dougalis, D. Mitsotakis, Numerical solution of KdV-KdV systems of Boussinesq equations: I. the numerical scheme and generalized solitary waves, *Mathematics and Computers in Simulation* 74 (2007) 214 – 228. doi:doi:10.1016/j.matcom.2006.10.004.
- [Iwasaki et al.(1990)Iwasaki, Toh, and Kawahara] H. Iwasaki, S. Toh, T. Kawahara, Cylindrical quasi-solitons of the Zakharov-Kuznetsov equation, *Physica D: Nonlinear Phenomena* 43 (1990) 293 – 303. doi:doi:10.1016/0167-2789(90)90138-F.
- [Nishiyama et al.(2012)Nishiyama, Noi, and Oharu] H. Nishiyama, T. Noi, S. Oharu, Conservative finite difference schemes for the generalized Zakharov-Kuznetsov equations, *Journal of Computational and Applied Mathematics* 236 (2012) 2998 – 3006. doi:doi:10.1016/j.cam.2011.04.010.
- [Zakharov and Kuznetsov(1974)] V. Zakharov, E. Kuznetsov, Three-dimensional solitons, *Soviet Physics JETP* 29 (1974) 594–597.

- [Xu and Shu(2005)] Y. Xu, C.-W. Shu, Local discontinuous Galerkin methods for two classes of two-dimensional nonlinear wave equations, *Physica D: Nonlinear Phenomena* 208 (2005) 21 – 58. doi:doi:10.1016/j.physd.2005.06.007.
- [Sanderse(2020)] B. Sanderse, Non-linearly stable reduced-order models for incompressible flow with energy-conserving finite volume methods, *Journal of Computational Physics* 421 (2020) 109736. doi:doi:https://doi.org/10.1016/j.jcp.2020.109736.
- [Reis and Stykel(2007)] T. Reis, T. Stykel, Stability analysis and model order reduction of coupled systems, *Math. Comput. Model. Dyn. Syst.* 13 (2007) 413–436. doi:doi:10.1080/13873950701189071.
- [Benner et al.(2020)Benner, Goyal, Kramer, Peherstorfer, and Willcox] P. Benner, P. Goyal, B. Kramer, B. Peherstorfer, K. Willcox, Operator inference for non-intrusive model reduction of systems with non-polynomial nonlinear terms, *Computer Methods in Applied Mechanics and Engineering* 372 (2020) 113433. doi:doi:10.1016/j.cma.2020.113433.
- [Benner et al.(2015)Benner, Gugercin, and Willcox] P. Benner, S. Gugercin, K. Willcox, A survey of projection-based model reduction methods for parametric dynamical systems, *SIAM Review* 57 (2015) 483–531. doi:doi:10.1137/130932715.
- [Ștefănescu et al.(2014)Ștefănescu, Sandu, and Navon] R. Ștefănescu, A. Sandu, I. M. Navon, Comparison of POD reduced order strategies for the nonlinear 2D shallow water equations, *International Journal for Numerical Methods in Fluids* 76 (2014) 497–521. doi:doi:10.1002/flid.3946.
- [Mahoney and Drineas(2009)] M. W. Mahoney, P. Drineas, CUR matrix decompositions for improved data analysis, *Proceedings of the National Academy of Sciences* 106 (2009) 697–702. doi:doi:10.1073/pnas.0803205106.
- [Karasözen et al.(2021)Karasözen, Yıldız, and Uzunca] B. Karasözen, S. Yıldız, M. Uzunca, Structure preserving model order reduction of shallow water equations, *Mathematical Methods in the Applied Sciences* 44 (2021) 476–492. doi:doi:10.1002/mma.6751.
- [Halko et al.(2011)Halko, Martinsson, and Tropp] N. Halko, P. G. Martinsson, J. A. Tropp, Finding structure with randomness: Probabilistic algorithms for constructing approximate matrix decompositions, *SIAM Review* 53 (2011) 217–288. doi:doi:10.1137/090771806.
- [Ohlberger and Rave(2016)] M. Ohlberger, S. Rave, Reduced basis methods: Success, limitations and future challenges, *Proceedings of the Conference Algorithmy* (2016) 1–12. URL: <http://www.iam.fmph.uniba.sk/amuc/ojs/index.php/algorithmy/article/view/389>.
- [Brugnano et al.(2019)Brugnano, Gurioli, and Sun] L. Brugnano, G. Gurioli, Y. Sun, Energy-conserving Hamiltonian boundary value methods for the numerical solution of the Korteweg-de Vries equation, *Journal of Computational and Applied Mathematics* 351 (2019) 117 – 135. doi:doi:10.1016/j.cam.2018.10.014.
- [Bo et al.(2020)Bo, Wang, and Cai] Y. Bo, Y. Wang, W. Cai, Arbitrary high-order linearly implicit energy-preserving algorithms for Hamiltonian PDEs, 2020. *arXiv:2011.08375*.
- [Liu and Yi(2016)] H. Liu, N. Yi, A Hamiltonian preserving discontinuous Galerkin method for the generalized Korteweg-de Vries equation, *Journal of Computational Physics* 321 (2016) 776 – 796. doi:doi:10.1016/j.jcp.2016.06.010.
- [Hairer et al.(2010)Hairer, Lubich, and Wanner] E. Hairer, C. Lubich, G. Wanner, Geometric numerical integration, volume 31 of *Springer Series in Computational Mathematics*, Springer, Heidelberg, 2010. Structure-preserving algorithms for ordinary differential equations, Reprint of the second (2006) edition.
- [Bona et al.(2008)Bona, Dougalis, and Mitsotakis] J. L. Bona, V. A. Dougalis, D. E. Mitsotakis, Numerical solution of Boussinesq systems of KdV-KdV type. II. Evolution of radiating solitary waves, *Nonlinearity* 21 (2008) 2825–2848. doi:doi:10.1088/0951-7715/21/12/006.